# Development of Silver-Nanoparticle-Based Planar Coil Electrode for Electromagnetic Cochlear Stimulation

Ressa Reneth Sarreal, Student Member, IEEE, and Pamela Bhatti, Senior Member, IEEE

Abstract— We present a planar coil electrode design for electromagnetic cochlear stimulation that utilizes silver nanoparticles and inkjet printing additive manufacturing techniques. These electrodes were designed in COMSOL, a finite element modeling tool, and fabricated using inkjet printing. The modelled micro coils have a maximum diameter of 600  $\mu m$ , a thickness of 1  $\mu m$ , and a trace width of 37.50  $\mu m$ . For ease of handling, coils that are scaled 100-times larger than the micro coils were modelled and fabricated. Radiation patterns were captured and analyzed. Approximately 4% error was observed between the model and the fabricated coils, validating the functionality of the fabricated coils.

#### I. INTRODUCTION

According to the National Institute on Deafness and other Communication Disorders (NIDCD) 2012 report, 324,000 people worldwide are cochlear implant users [1], and the number of users is increasing steadily. A cochlear implant replaces the function of hair cells located within the inner ear when these cells are damaged or lost. The snail-like structure of the cochlea spatially filters acoustic waves based on their frequencies (Fig. 1). The hair cells located throughout cochlea transduce the obtained acoustic waves into an electrical signal that traverses through the nervous system; thus, without the cells, hearing functionality is imperfect or impossible. A cochlear implant bridges the gap caused by non-functional hair cells, then a chain of action potentials, electrical signals produced by nearby neurons, may trigger. Currently, cochlear implants directly inject electrical current into surrounding tissue, which causes action potentials to fire; however, recent studies have shown that utilizing electromagnetic fields to stimulate nearby tissue [2], rather than direct current injection, can improve spatial resolution of the tissue in the cochlea [3] and improve the functionality of a cochlear implant [4].



Fig. 1. The anatomy of the human ear (courtesy: Encyclopedia Britannica, Inc.).

\*Research supported in part by the National Science Foundation under Grants CAREER ECCS-1055801, ECCS #1809334, and PFI-TT #1827321.

R. Sarreal is a PhD student at the Georgia Institute of Technology, School of Electrical and Computer Engineering, Atlanta, GA 30312 USA (corresponding author to provide e-mail: rsarreal3@gatech.edu).

# II. METHODOLOGY

#### A. Finite Element Modeling

Using COMSOL Multiphysics (COMSOL, Inc.; Burlington, MA, USA). the coils are designed as a half-Archimedean pattern, shown in Fig. 2, with an inner radius of 60  $\mu m$ , and an outer radius of 600  $\mu m$ . The trace width is kept constant at 37.50  $\mu m$ , while the thickness of the entire coil is 1  $\mu m$ . The following formulas were utilized to generate the coil pattern:

$$b = \frac{r_f - r_i}{\theta_f} \tag{1}$$

$$r_k = r_i + b\theta_k \tag{2}$$

$$x_k = r_k \cos(\theta_k) \tag{3}$$

$$y_k = r_k \sin(\theta_k) \tag{4}$$

Where b is a constant dependent on  $r_i$ , the initial inner radius,  $r_f$ , the final outer radius,  $\theta_f$ , the terminal angle of the coil, relative to the initial angle of the coil, 0 degrees. A combination of all discrete incremental coordinate pairs,  $(x_k, y_k)$ , completes the outline of the spiral. A trace width of 37.50  $\mu$ m is applied to the outline, such that the outline perfectly bisects the width.

## B. Inkjet Printing

Inkjet printing is an additive manufacturing technique that utilizes inexpensive, commercially available products when compared to common MEMS microfabrication techniques. The printer utilized is the Epson Stylus C88+Inkjet Printer (Epson America, Inc.; Long Beach, CA, USA), the substrate used is the Novele IJ-200 PET-based (NovaCentrix; TX, USA) printed electronics substrate [5],

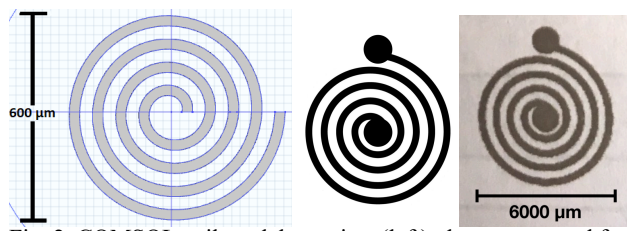


Fig. 2. COMSOL coil model top view (left), the pattern used for the planar coil electromagnetic electrodes (middle), and an inkjet-fabricated coil (right).

P. Bhatti, PhD, is an Associate Professor at the Georgia Institute of Technology, School of Electrical and Computer Engineering, Atlanta, GA 30312 USA (corresponding author to provide e-mail: pbhatti@ece.gatech.edu).

and the silver ink is comprised of the Metalon JS-B25P nano-silver ink by NovaCentrix with a 75 nm diameter particle size.

The printer was prepared using NovaCentrix protocol to fully utilize conductive, silver ink rather than the intended commercial printer ink. A basic coil pattern is designed, shown in Fig. 2., and saved as a .png or .dwg file. The print has a one micron thickness [6], and was allowed a 24-hour resting period at 25°C prior to any handling for best results.

For ease of handling, the printed coils are scaled 100-times larger than the originally modelled micro coils. These larger coils were also modelled in COMSOL to verify identical behavior to the micro coils, with scaled driving frequency, as defined in the next section.

## C. Experimental Testing

The testing environment is comprised of a signal generator (Rohde & Schwarz; Munich, Germany), oscilloscope (Rohde & Schwarz, Munich, Germany), 50  $\Omega$  Bayonet Neill-Concelman (BNC) cables, acrylonitrile-butadiene-styrene (ABS) -based support structure, and faraday cage to prevent any interference from external sources.

The radiation pattern between two identical coils was captured with the following procedure. One coil was designated as the transmitter, and the other coil was designated as the receiver. The receiver, connected to an oscilloscope, was positioned 20 cm from the transmitter to emulate the 2 mm diameter of the cochlear structure [7], scaled up 100 times. The transmitter coil was rotated at 10-degree increments, and voltage was measured at the receiver coil. The process was repeated until the transmitter coil had rotated a complete 360 degrees. The bandwidths for the coils (Table 1) were calculated using the following equations:

$$v_p = \frac{c}{\sqrt{\varepsilon_r \mu_r}} \tag{5}$$

$$\lambda = \frac{v_p}{f} \tag{6}$$

Where  $v_p$ , propagation velocity, is dependent on the relative permittivity and permeability of the propagation material,  $\varepsilon_r$  and  $\mu_r$  respectively. c is the speed of light in a vacuum. The wavelength,  $\lambda$ , is equivalent to a circumference of a spiral loop, and f is the driving frequency. The bandwidth was calculated using the circumferences of the smallest and largest loops in the coil.

<u>Table 1: Bandwidth for Coils of Varying Size in Free Space and Phosphate-Buffered Saline (PBS)</u>

Coil Diameter (µm)	Air/Free Space	PBS
60000	1.60 GHz -15.95 GHz	56.33 MHz - 563.25 MHz
600	159.50 GHz - 1595.00 GHz	5.63 GHz - 56.30 GHz

Driving frequencies were selected based on the available equipment. A 1.6 GHz sinusoidal signal with an amplitude of 500 mV was inputted into the transmitter.

# III. RESULTS

To compare the radiation patterns, the amplitudes were scaled down by the respective maximum amplitudes; therefore, the compared values are limited from zero to one mV/mV. A 3.3% error between the rear lobe magnitudes of

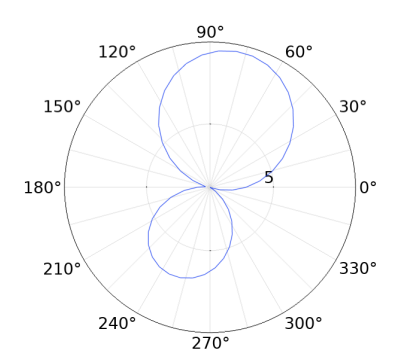


Fig. 4. Far-field radiated field pattern (V/m) obtained from the COMSOL model simulation.

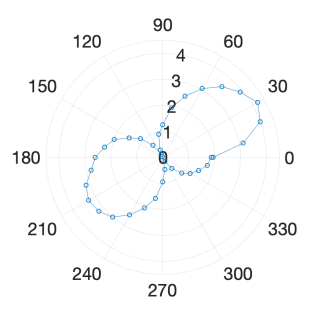


Fig. 5. Experimental radiated pattern (mV) generated in the far-field zone. The resulting pattern is an average between four experimental trials.

the COMSOL simulation pattern (0.8125), shown in Fig. 4, and experimental data (0.7857), shown in Fig. 5, was observed. The radiation patterns are similar such that, relative to the main lobe, the minima and rear lobe occur at the same angular locations. Power loss between transmitter (3.14 mW) and receiver (1.57 uW) coil is approximately 99.5% of the input supply.

#### ACKNOWLEDGMENT

Guidance was provided by Dr. Waymond Scott at the Georgia Institute of Technology, School of Electrical and Computer Engineering.

#### REFERENCES

- The national institute on deafness and other communication disorders statistics, https://www.nidcd.nih.gov/health/cochlearimplants
- [2] G. Bonmassar, S. W. Lee, D. K. Freeman, M. Polasek, S. I. Fried, and J. T. Gale, "Microscopic magnetic stimulation of neural tissue," Nature Communications, vol. 3, no. 921, 2012.
- [3] S. Mukesh, D. T. Blake, B. J. McKinnon, and P. T. Bhatti, "Modeling Intracochlear Magnetic Stimulation: a Finite-Element Analysis", *IEEE Trans Neural Syst Rehabil Eng.*, vol. 25, no. 8, pp. 1353-1362, 2016.
- [4] S. Mukesh, R. Zeller-Townson, R. Butera, and P. Bhatti, "Magnetic Stimulation of Dissociated Cortical Neurons on a Planar Multielectrode Array", *IEEE EMBS Conference on Neural Engineering*, San Fransisco, CA, Mar. 2019.
  [5] NovaCentrix, "Novele Printing Media", online:
- https://store.novacentrix.com/Novele-IJ-220-p/910-0070-02.htm, 2019.
- [6] S. Jiang, "Inkjet Printing of Nano-Silver Conductive Ink on PET Substrate", online: https://pdfs.semanticscholar.org/ee19/194816afef96d943f1d285bdd 6877b5a9c5c.pdf, 2017.
- [7] J. Hawkins, "Human Ear", Encyclopedia Britannica, inc., online: https://www.britannica.com/science/ear/Cochlea, 2018.